International Journal of Luminescence and applications
Vol6 (1) February, 2016, pages 52-57

STRUCTURAL CHARACTERIZATION AND OPTICAL PROPERTIES OF Eu^{2+} AND Dy^{3+} DOPED Sr_2SiO_4 PHOSPHOR BY SOLID STATE REACTION METHOD

Durga Verma, R.P.Patel[1], Mohan L.Verma, Upma
Department of Applied Physics, Faculty of Engineering and Technology, Shri Shankaracharya Group of Institutions, Shri Shankaracharya Technical Campus, Bhilai (C.G.) 490020, India
[1]Department of Applied Physics, Professional Institute of Engineering and Technology, Raipur (C.G.) 492001, India
Email Id: dbanchhor16@gmail.com

Abstract
Dysprosium and europium doped strontium silicate (Sr_2SiO_4) phosphors were synthesized using high-temperature solid-state reaction technique. The obtained phosphor was characterized by powder X-ray diffraction, scanning electron microscopy, FTIR, UV–visible spectroscopy and thermoluminescence. From scanning electron microscopy (SEM), agglomerations of particles were observed. The chemical composition of the prepared $Sr_2SiO_4:Eu^{2+}$ and $Sr_2SiO_4:Dy^{3+}$ phosphors were confirmed by energy dispersive X-ray spectroscopy (EDX). Thermoluminescence study carried out on the phosphor with UV irradiation showed one glow peak. The trapping parameters associated with the glow peak of $Sr_2SiO_4:Eu^{2+}$ and $Sr_2SiO_4:Dy^{3+}$ were determined using Chen's glow curve method.
Keyword: *- solid state reaction, spectroscopy, SEM, FTIR, Termoluminescence.*

INTRODUCTION

Currently there is a great deal of interest optical and structural properties of nanometer sized semiconductor particle or thin films [1]. Since the mid 1990s, persistent luminescence materials have received exceptional attention not only due to their versatile applications, but also because of the scientific challenges offered by the phenomenon itself. The various applications extend from the common place luminous paints and ceramics for e.g. emergency signals to highly sophisticated uses in micro defect sensing, optoelectronics for image storage and high energy radiation detection as well as in pressure/temperature sensing.

The chemical and physical properties of inorganic micro/nano structured materials are dependent on their chemical composition, size, morphology, phase and also dimensionality of the crystal [2–5]. Therefore, in the past decade, extensive research work was devoted to have control over these parameters [6]. More applications and novel functional materials might emerge, if shape-controlled nano/micro crystals could be achieved with high complexity [7]. Rare-earth ion-doped inorganic luminescent materials have considerable applications in most devices for artificial light production [8]. Phosphors are composed of an inert host lattice and an optically excited activator, typically of 3d or 4f metal ions. Usually, inorganic luminescent materials are applied in displays such as television tubes, computer monitor, oscilloscopes, radar screens and displays in electron microscopes [9]. One of the yellow emitting afterglow phosphors is strontium ortho-silicate (Sr_2SiO_4) doped with Eu^{2+} and Dy^{3+}. The Eu^{2+} activated ortho-silicates were first reported by Barry [10] and Blasse et al. in 1968 [11] and were intensively studied as phosphors for color-tunable white light emitting diodes (LEDs). The luminescence of divalent europium doped ortho-silicate is attributed to the $[Xe]4f^6\ 5d^1$-$[Xe]4f^7$ transition and is strongly influenced by the local coordination in the host lattice [12]. In recent times, Dy^{3+} doped ortho-silicate (Sr_2SiO_4: Dy^{3+}) powers were fascinated due to its excellent emission characteristics, single luminescent center and high absorption efficiency in the UV region [13].

Thermoluminescence (TL) is observed when, in the process of irradiating a material, part of the irradiation energy is used to transfer electrons to traps. This energy, stored in the form of the trapped electrons, is released by raising the temperature of the material, and the released energy is converted to luminescence. The trapping process and the subsequent release of the stored energy find important application in ionizing radiation dosimetry and in the operation of long persistence phosphors. The shape and position of the TL glow curves can be analyzed to extract information on the various parameters of the trapping process—trap depth, trapping and re-trapping rates, etc. TL finds wide applications in radiation dosimetry, archeological dating, mineral prospecting, forensic science etc. [14].

Solid-state reaction method is usually used to prepare $Sr_2SiO_4:Eu^{2+}$ and $Sr_2SiO_4:Dy^{3+}$ phosphors. In this method, the reactants are mixed thoroughly and the mixture is then heated or fired under an appropriate atmosphere. To facilitate the reaction and to improve the crystalline of the luminescent materials, flux agents or molten salts are often added to provide a more interactive medium for the reaction [15].

In the present study, we report the synthesis of europium and dysprosium doped strontium silicate phosphor by high

temperature solid state reaction method. This report describes the structural characterization on the basis of XRD, SEM, energy band gap and TL study of $Sr_2SiO_4:Eu^{2+}$ and $Sr_2SiO_4:Dy^{3+}$ phosphors.

2. EXPERIMENTAL DETAILS

2.1 Synthesis

Solution solid state reaction technique was employed for the preparation of Sr_2SiO_4: Eu^{2+} and Sr_2SiO_4: Dy^{3+} phosphor. Strontium nitrate [$Sr(NO_3)_2$ (99.99%)], silica gel (99.99%)], and Rare-earth material dysprosium oxide [Dy_2O_3 (99.99%)] and europium oxide [Eu_2O_3 (99.99%)], all of analytical reagent (A.R.), grade, were employed in this experiment. Ammonium chloride (NH_4Cl) was used as flux. Initially, the raw materials were weighed according to the nominal compositions of [2Sr $(NO_3)_2$ - silica gel - NH_4Cl - 1%RE (Dy_2O_3, Eu_2O_3)] Sr_2SiO_4: Eu^{2+} and Sr_2SiO_4: Dy^{3+} phosphor. Then the powders were mixed and milled thoroughly for 2 h. using mortar and pestle. The ground sample was placed in an alumina crucible and subsequently fired at 1200^0C for 3 h. At last the nominal compounds were obtained after the cooling down of programmable furnace.

2.2 Characterization techniques

Crystal structure and phase formation of the phosphors were examined using an X-ray diffractometer (Philips PAN Analytical X'pert Pro) operating at 40 kV and 30mA with CuKα radiation (λ=1.54056 Å) and data collected over the 2θ range $20\text{-}60^0$. The surface morphology of prepared phosphors was determined by the SEM (ZIESS EVO-18) operated at the acceleration voltage of 5 kV. The samples were coated with a thin layer of gold (Au) and then surface morphology of prepared was observed. Energy dispersive x-ray spectroscopy (EDX) was used for the elemental (quantitative and qualitative) analysis of the prepared phosphor. Absorption spectra were recorded using Shimadzu UV-1700 UV-Visible spectrophotometer. A routine TL setup (Nucleonix TL 10091) was used for recording TL glow. The samples were irradiated with UV-rays source. Thermoluminescence were studied with PC based Thermoluminescence analyzer (10091) system set-up.

3. RESULT AND DISCUSSION

3.1 X-ray diffraction analysis

X-ray diffraction (XRD) analysis was used to characterize the synthesized phosphors. The analysis of XRD data of Sr_2SiO_4 phase is usually qualitative, based on relative peak intensities. Strontium silicate exists in monoclinic (β-Sr_2SiO_4) phase at low temperatures and in orthorhombic (α'-Sr_2SiO_4) phase at high temperatures with a transition temperature of ~85^0C. It has been reported that the crystal structure of α'-Sr_2SiO_4 (orthorhombic), and β-Sr_2SiO_4 (monoclinic) are similar [16].

The typical X-ray diffraction patterns of the resultant $Sr_2SiO_4:Eu^{2+}$ and $Sr_2SiO_4:Dy^{3+}$ are shown in Figure 1. The XRD pattern for the pure (undoped) Sr_2SiO_4 is also given for comparison. The orthorhombic phase diffraction peaks of the pure Sr_2SiO_4 were clearly observed in the XRD patterns. The XRD patterns were similar for all the prepared samples and the peak positions are unchanged with change in doping element. The position and intensity of diffraction peaks of every sample were matched and could be indexed to the orthorhombic phase of α'-Sr_2SiO_4 (COD card No. **98-003-5667**). These results revealed that the crystal structure of the phosphor has not changed, though the $Eu^{2+}$and Dy^{3+} ions occupy Sr^{2+} sites within the Sr_2SiO_4 phosphor, because the ionic radius of Sr^{2+} (1.21 A^0) nearly matches with the Eu^{2+} (1.20 A^0) and Dy^{3+} (0.99 A^0) ionic radius.

XRD data was indexed on an orthorhombic system with space group Pnma having cell parameters a= 7.0900 A^0, b= 5.6820 A^0 and c= 9.7730 A^0. An estimation of average crystalline size for the sample was done using Debye Scherrer's formula [17],

$$L=0.94\lambda/\beta\cos\theta$$

where L is the crystalline size, λ is the wavelength (for Cu Kα, λ=1.5406 A^0), β is the full width at half maximum (FWHM) and θ is the Bragg's angle. As shown in Figure 1, the principal diffraction peaks are at 2θ= 30.6, 31.2, 31.8. The crystalline size using Debye Scherrer's formula of $Sr_2SiO_4:Eu^{2+}$ and $Sr_2SiO_4:Dy^{3+}$ were calculated to be about 31 nm and 27 nm respectively.

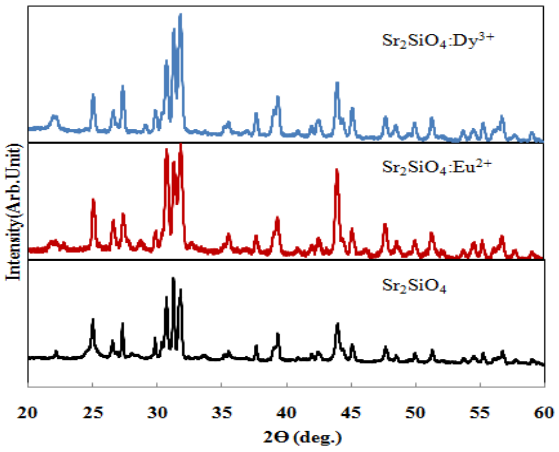

Fig.1: XRD pattern of $Sr_2SiO_4:Eu^{2+}$ and $Sr_2SiO_4:Dy^{3+}$ phosphors.

3.2 Morphological characterization: scanning electron microscopy

SEM study was carried out to investigate the surface morphology and the crystalline size of the synthesized phosphors. Figure 2(a-d) shows the representative SEM micrographs taken for $Sr_2SiO_4:Eu^{2+}$ and $Sr_2SiO_4:Dy^{3+}$ (1% mol Eu and 1% Dy) at different magnifications(x2000 and x10000) respectively. The surface morphology of the particles was not uniform and they aggregated tightly with one another. In addition, the agglomeration of particles is expected in phosphor prepared by high temperature solid state reaction method. From Figure 2(a-d) of the SEM image, it can be observed that the prepared sample consists of particles with different size distribution.

3.3 Energy dispersive X-ray spectroscopy (EDX)

Figure 3(a, b) shows the EDX spectra of $Sr_2SiO_4:Eu^{2+}$ and $Sr_2SiO_4:Dy^{3+}$ phosphor. The composition of the powder sample has been measured using EDX. The existence of Europium (Eu) and Dysprosium (Dy) in prepared phosphors is clear in their corresponding EDX spectra. There is no other peak apart from strontium (Sr), silicon (Si), oxygen (O), Europium (Eu) / dysprosium (Dy) in $Sr_2SiO_4:Eu^{2+}$/ $Sr_2SiO_4:Dy^{3+}$ EDX spectra of the samples.

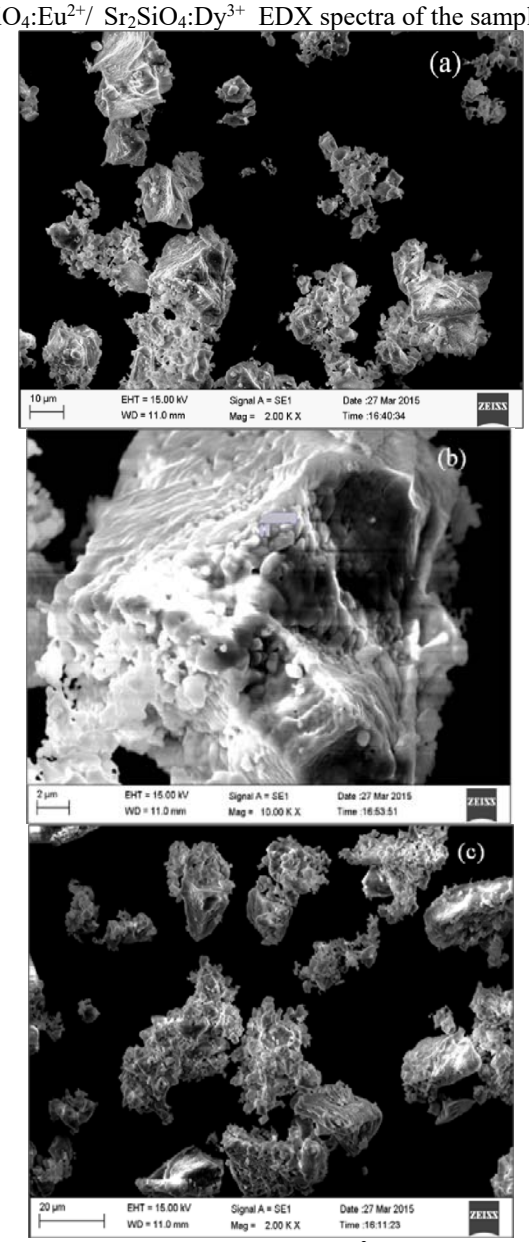

Fig.2:- SEM micrograph of $Sr_2SiO_4:Eu^{2+}$ (a, b), $Sr_2SiO_4:Dy^{3+}$ (c, d) phosphor with different magnification.

In the EDX spectrum 3(a), the presence of Sr, Si, O and Eu, intense peaks are present, which confirm the presence of elements in prepared $Sr_2SiO_4:Eu^{2+}$ phosphor and EDX spectrum 3(b), the presence of Sr, Si, O and Dy intense peaks are present, which confirm the presence of elements in prepared $Sr_2SiO_4:Dy^{3+}$ phosphor.

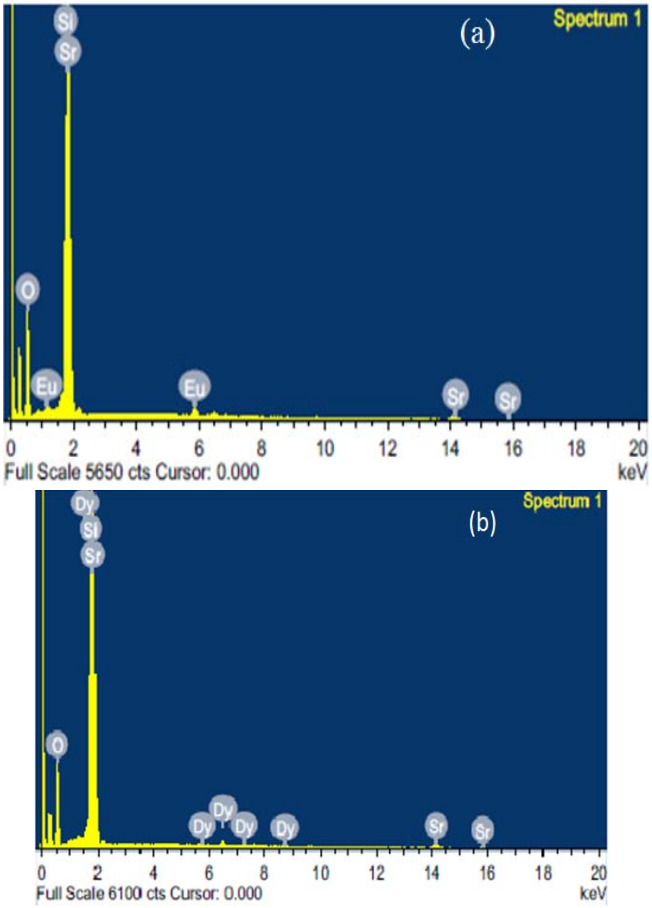

Fig. 3:- EDX spectra (a) $Sr_2SiO_4:Eu^{2+}$ (b) $Sr_2SiO_4:Dy^{3+}$ phosphor

3.4 Optical Absorption Spectra

The optical absorption spectra can be used as a good quality check for the optical behavior of materials. UV-visible spectrum gives information about the excitonic transition of nano materials [18]. In Figure 4, the optical absorption spectra of $Sr_2SiO_4:Eu^{2+}$ and $Sr_2SiO_4:Dy^{3+}$ is shown in the range of 200-500 nm. It can be seen that the absorption edges are found at λ= 213 nm wavelength and λ= 215 nm. The band gap energy can be determined using the Tauc relation [19-22]. In the Tauc plot graph between $(\alpha h\upsilon)^2$ versus photon energy, the extrapolation of the straight line $(\alpha h\upsilon)^2=0$, gives the value of band gap (Figure 5).

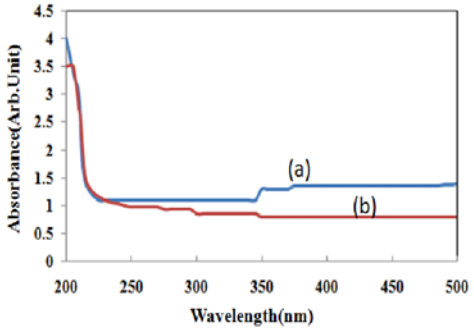

Fig.4: - Absorption spectra of (a) $Sr_2SiO_4:Eu^{2+}$ (b) $Sr_2SiO_4:Dy^{3+}$ phosphor.

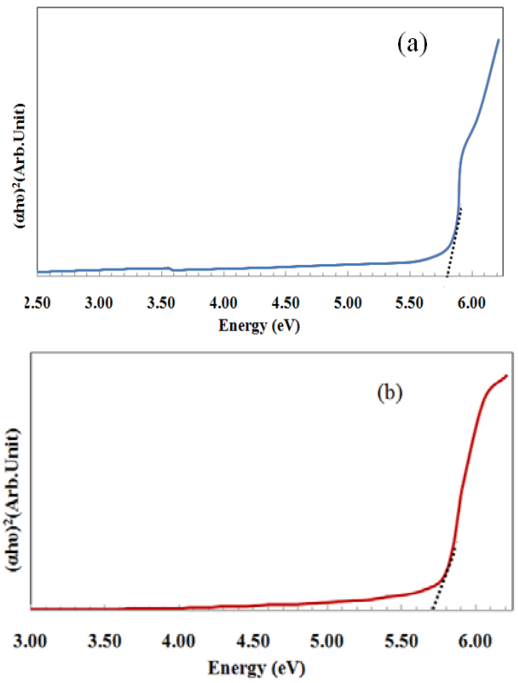

Fig.5: - Tauc Plot of (a) $Sr_2SiO_4:Eu^{2+}$ (b) $Sr_2SiO_4:Dy^{3+}$ phosphor.

From the UV spectra, it is clear that the absorbance decreases with increase in wavelength. This increase in transmittance indicates the presence of optical band gap in the material. The calculated band gap value for $Sr_2SiO_4:Eu^{2+}$ is 5.8eV and for $Sr_2SiO_4:Dy^{3+}$, it is 5.7eV.

3.5 Thermoluminescence Studies

Thermoluminescence is thermally stimulated emission of light from an insulator or semiconductor following the previous absorption of energy from ionizing radiation [23-25]. TL glow curves of UV-rays irradiated Sr_2SiO_4 phosphors for $Eu^{2+}$and Dy^{3+} dopants are shown in Figure 6(a) and 6(b) at a heating rate 5^0C/s. A single glow peak was observed for both dopants, though the temperature of the peak was different. The variation of TL glow peak intensity with increasing time (min.) of UV exposure was plotted for both the dopants (Figure 7). It was observed that intensity increases with increasing UV exposure. Further it was found that TL intensity is more in $Sr_2SiO_4:Dy^{3+}$ sample.

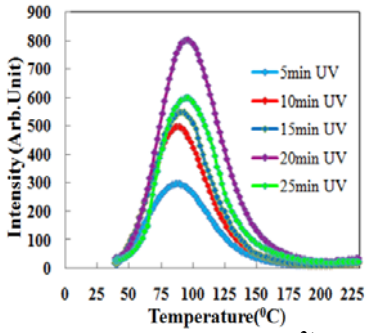

Fig. 6(a): - TL glow peak of $Sr_2SiO_4:Eu^{2+}$ phosphor with increasing UV exposure time (min).

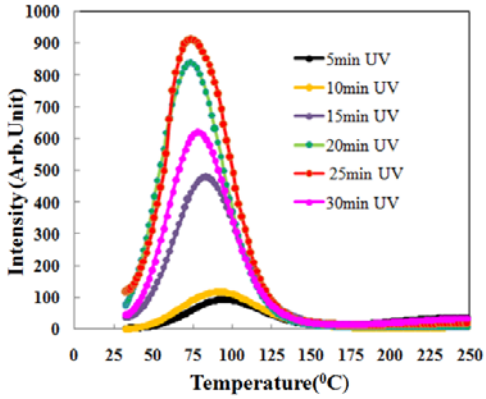

Fig. 6(b): - TL glow peak of $Sr_2SiO_4:Dy^{3+}$ phosphor with increasing UV exposer time (min).

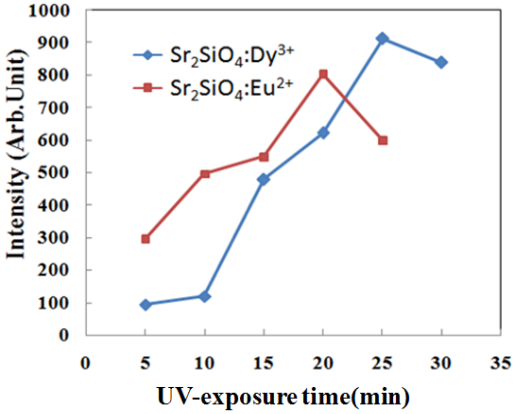

Fig. 7:- Variation of TL peak intensity with increasing UV exposure time(min).

In $Sr_2SiO_4:Eu^{2+}$ phosphor, thermoluminescence signal intensity is maximum for 20 min. of UV exposure and $Sr_2SiO_4:Dy^{3+}$ phosphor, thermoluminescence signal intensity is maximum for 25 min. of UV exposure, after which it starts to decrease. The charge carrier density might be increasing with increasing UV exposure, but after some time of exposure, trap level may have started to destroy resulting in decrease in thermoluminescence signal.

TL glow peak temperature and intensity depends on various parameters such nature of the host, dopant, type of ionizing radiation, and amount of irradiation and environment of the sample during measurement, temperature at which the measurements are carried out, purity of the sample, heating rate etc. [26]. Figure 8 shows TL glow curve of pure, $Sr_2SiO_4:Eu^{2+}$ and $Sr_2SiO_4:Dy^{3+}$ phosphor with highest intensity of signal. In un-doped Sr_2SiO_4 phosphor, TL intensity is negligible as compared to Eu^{2+} and Dy^{3+} doped Sr_2SiO_4 phosphors.

International Journal of Luminescence and applications
Vol6 (1) February, 2016, pages 52-57

Sample Name	Heating Rate(^{0}C/s)	T_1(^{0}K)	T_m(^{0}K)	T_2(^{0}K)
$Sr_2SiO_4:Eu^{2+}$	5	348.2	367.7	400.5
$Sr_2SiO_4:Dy^{3+}$	5	328	348.7	385

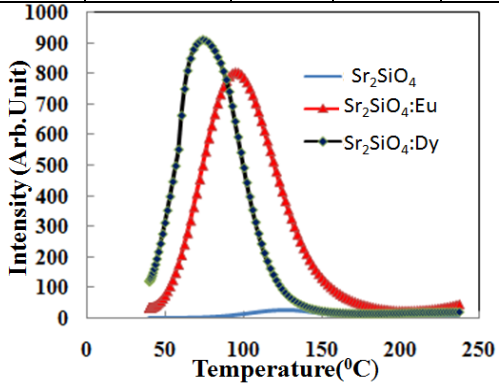

Fig.8:- TL glow peak of Un-doped and doped (Eu^{2+} and Dy^{3+}) Sr_2SiO_4 phosphor.

An isolated single peak is observed due to only one type of luminescence centre is formed of samples. In Dy^{3+} doped in host materials, TL peak was observed around 75.68^{0}C and TL peak observed around 94.67^{0}C of Eu^{2+} doped Sr_2SiO_4 phosphor.

The TL parameter, the thermal activation energy E (the trap depth) is obtained using peak shape method [27-29]. The kinetic order can be related to the geometrical factor (μ_g) by the relation $\mu_g = \delta/\omega = T_2-T_m / T_2-T_1$ where T_1 and T_2 represent respectively the temperatures of half intensity at low temperature side peak temperature and high temperature side of TL peak and T_m is the peak temperature at the maximum TL intensity and $\delta = T_2-T_m$, $\tau = T_m-T_1$ and $\omega = T_2-T_1$, therefore, E_δ, E_τ and E_ω are the corresponding activation energy. As per μ_g value, Sr_2SiO_4 with different dopant phosphor shows the general order of kinetic and the activation energy is given by

$$E_\alpha = C_\alpha\left(\frac{kT_m^2}{\alpha}\right) - b_\alpha(2kT_m)$$

For general order kinetics, the values of the c_α and b_α ($\alpha = \tau, \delta, \omega$) are calculated

$c_\tau = [1.51+3(\mu g - .42)]$, $b_\tau = [1.58+4.2((\mu g -0 .42)]$

$c_\delta = [0.976+7.3(\mu g -0 .42)]$, $b_\delta = 0$ and

$c_\omega = [2.52+10.2(\mu g - 0.42)]$, $b_\omega = 1.0$

The relationship between the frequency factor's' and the depth of the trap 'E' is given by the following equation [30]

$$\frac{\beta E}{kT_m^2} = s\left[1+(b-1)\frac{2kT_m}{E}\right]\exp(-E/kT_m)$$

where k is Boltzmann constant, E is activation energy, b is order of kinetics, T_m is the peak temperature at the maximum TL intensity and β is the heating rate. In the present work, $\beta = 5^0$C/s.

Table1:- Values of different parameters calculated from TL glow curves

τ	δ	ω	$\mu_g=\delta/\omega$	Activation Energy (eV)	Frequency Factor 'S'(s^{-1})
19.47	32.83	52.3	0.52	0.99	1.67 x10^{13}
18.76	28.24	47	0.50	0.91	8.18 x10^{12}

Theoretically, the values of symmetry factor (μ_g) for first and second order kinetics are close to 0.42 and 0.52, respectively. The activation energy (E_α) or trap depth which is the thermal energy required to liberate the trapped electron and holes can be determined by the Chen's equation. Kinetic parameters calculated from glow curves are presented in Table 1. The value of trap depth, which resembles the activation energy, is calculated to 0.99 and 0.91eV. It is worth reporting that the shape factor, which is 0.52 and 0.50, shows the second order kinetics and supports the probability of re-trapping released charge carriers before recombination. The afterglow of any phosphor is generated by the deeper trapped carriers, which recombine with the opposite carriers in the luminescent center with a transition resulting in the long afterglow [31].

4. CONCUSION

In this work, $Sr_2SiO_4:Eu^{2+}$ and $Sr_2SiO_4:Dy^{3+}$ phosphors were prepared by solid state reaction method. From XRD studies, a single orthorhombic phase was achieved. The average crystallite size of $Sr_2SiO_4:Eu^{2+}$ phosphor is ~31 nm and $Sr_2SiO_4:Dy^{3+}$ phosphor is ~27 nm. From SEM studies, in both phosphors, the particles appear to be non uniform and agglomerates composed of circular with several micrometers in size. The EDX spectra confirm the present elements in phosphors. The absorption spectra of Sr_2SiO_4 phosphor doped with Eu^{2+} / Dy^{3+} shows wide band gap. The TL glow curve for Eu^{2+}/ Dy^{3+} doped Sr_2SiO_4 phosphors exhibits an isolated glow peak, due to only one type of luminescence centre. Calculated glow peak parameters of the phosphor indicate that obey second order kinetics.

ACKNOWLEDGEMENT

We gratefully acknowledge the kind support of the management of Shri Shankaracharya Group of Institutions (SSTC). Authors also thank the Department of Metallurgical Engineering, NIT Raipur for help in the XRD and Scanning Electron Microscopy (SEM) analysis of samples.

References

1. R. Banerjee, R. Jayakrishnan, P Ayyub, J Physics Condens Matter 12 (2000) 10647.
2. Ajay Singh, Robert D. Gunning, Shafaat Ahmed, Christopher A. Barrett, Niall J. English, Jos-Antonio

Garatea, Kevin M. Ryan, J. Mater. Chem. 22 (2012) 1562.
3. L.Z. Pei, Y.Q. Pei, Y.K. Xie, C.Z. Yuan, D.K. Li, Qian-Feng Zhang, CrystEngComm 14 (2012) 4262.
4. Parada Siriwong, Titipun Thongtem, Anukorn Phuruangrat, Somchai Thongtem, CrystEngComm 13 (2011) 1564.
5. Shaohua Huang, Jie Xu, Zhenguo Zhang, Xiao Zhang, Liuzhen Wang, Shili Gai, Fei He, Na Niu, Milin Zhang, Piaoping Yang, J. Mater. Chem. 22 (2012) 16136.
6. H. Dong, X. Li, J.Q. Peng, X. Wang, J.P. Chen, Y.D. Li, Angew. Chem. Int. Ed 44 (2005) 2782.
7. E.C Hao, R.C. Bailey, G.C Schatz, J.T. Hupp, S.Y. Li, Nano Lett. 4 (2004) 327.
8. T. Justel, H.Nikol,C. Ronda, 1998Angewandte Chemie International Edition 37 (1998)3085-3103.
9. C. Feldmann,T. Jüstel,C.R. Ronda,P.J.Schmidt,Adv. Funct. Mater. 13(2003) 511-516.
10. T.L.Barry, J. Electrochem.Soc. 115 (1968) 1181-1184.
11. G.Blasse, W.L. Wanmaker, J.W. ter Vrugt, A. Bril, Philips Res. Rep. 23 (1968) 189-200.
12. G. Blasse, B.C. Grabmaier, Luminescent Materials, Springer-Verlag, Berlin(1994)DOI : 10.1007/978-3-642-79017-1.
13. L.Zhang,Z.Lu,H.Yang,P.Han,N.Xu,Q.Zhang,J.Alloys Compd.512 (2012) 5-11.
14. A.A.Braner, M.Israeli, Phys. Rev. 132(1963) 2501–2505.
15. J.H.Lee,Y.J. Kim,Journal of Ceramic Processing Research 10(2009) 81-84.
16. M.Catti , G.Gazzoni , G.Ivaldi , G.Zanini, Acta Crystallographic, Section B: B39(1983)674-679.
17. L.Stenberg ,B.G.Hyde ,Acta Crystallographica Section B : Structural Science , B42(1986)417-422.
18. B.Choudhury,M.Dey,A.Choudhury 2013, International Nano Letters, springer open journals, 3:25(2013)1-8.
19. J.Tauc,A. Menth, Journal of Non-Crystalline Solids, 8–10(1972)569–585.
20. J.Tauc,Materials Research Bulletin, 3(1968) 37–46.
21. J.Tauc,R.Grigorovici,A.Vancu, Physica Status Solidi (b), 15(1966) 627-637.
22. D.B.Buchholz,J.Liu,T.J.Marks,M.Zhang,R.P.H.Chang, ACS Appl. Mater. Interfaces, 1*(2009)* 2147-2153.
23. A.Pandey, R.G.Sonkawade and P.D.Sahare, Journal of physics D.Applied Phys 35 (2002) 2744-2747.
24. Surender Singh,S.P.Lochab,Ravi kumar and Nafa Sing,Physica B 406(2011)177-180.
25. K.S.Chung,H.S.Choe, J.I.Lee and J.L.Kim,Radiation materials 42(2007) 731-734.
26. N.Dhananjaya, H.Nagabhushana, B.M. Nagabhushana, B.Rudraswamy,C.Shivakumara,K.P.Ramesh, R.P.S. Chakradhara, physica B 406 (2011) 1645-1652.
27. R.Chen,Journal of Electrochemical Society: Solid state Science, 116(1969)1254-1257.
28. M.Gökçe, K.F.Oguz, T.Karalı,M.Prokic,Journal of physics D: Applied Physics.,42(2009) 105412-105416.
29. Z.X.Yuan, C.K.Chang, D.L.Mao,W.Ying, Journal of Alloys and Compounds, 377(2004) 268–271.
30. V.Pagonis,G.Kitis,C.Furetta, Springer Science Business Media, 8(2006) 32-33.
31. R.Chen,S.W.S.McKeever,"Theory of Thermo luminescence and Related Phenomena", World Scientific, Singapore 1997.